Supporting Information for

Divergent Responses of Historic Rain-on-Snow Flood Extremes to a Warmer Climate

Dalei Hao, Gautam Bisht, Donghui Xu, Mukesh Kumar, L. Ruby Leung

Corresponding author: Dalei Hao
Email: dalei.hao@pnnl.gov

This PDF file includes:

Figures S1 to S16
Tables S1 to S3
SI References

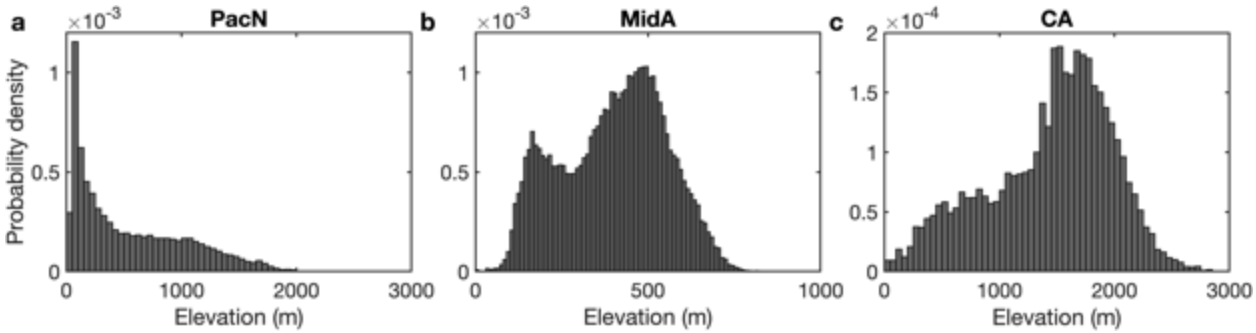

Supplementary Figure 1. Histograms of surface elevation for the three study domains in the Pacific Northwest (PacN) region, Mid-Atlantic (MidA) region, and California (CA), over the Contiguous United States.

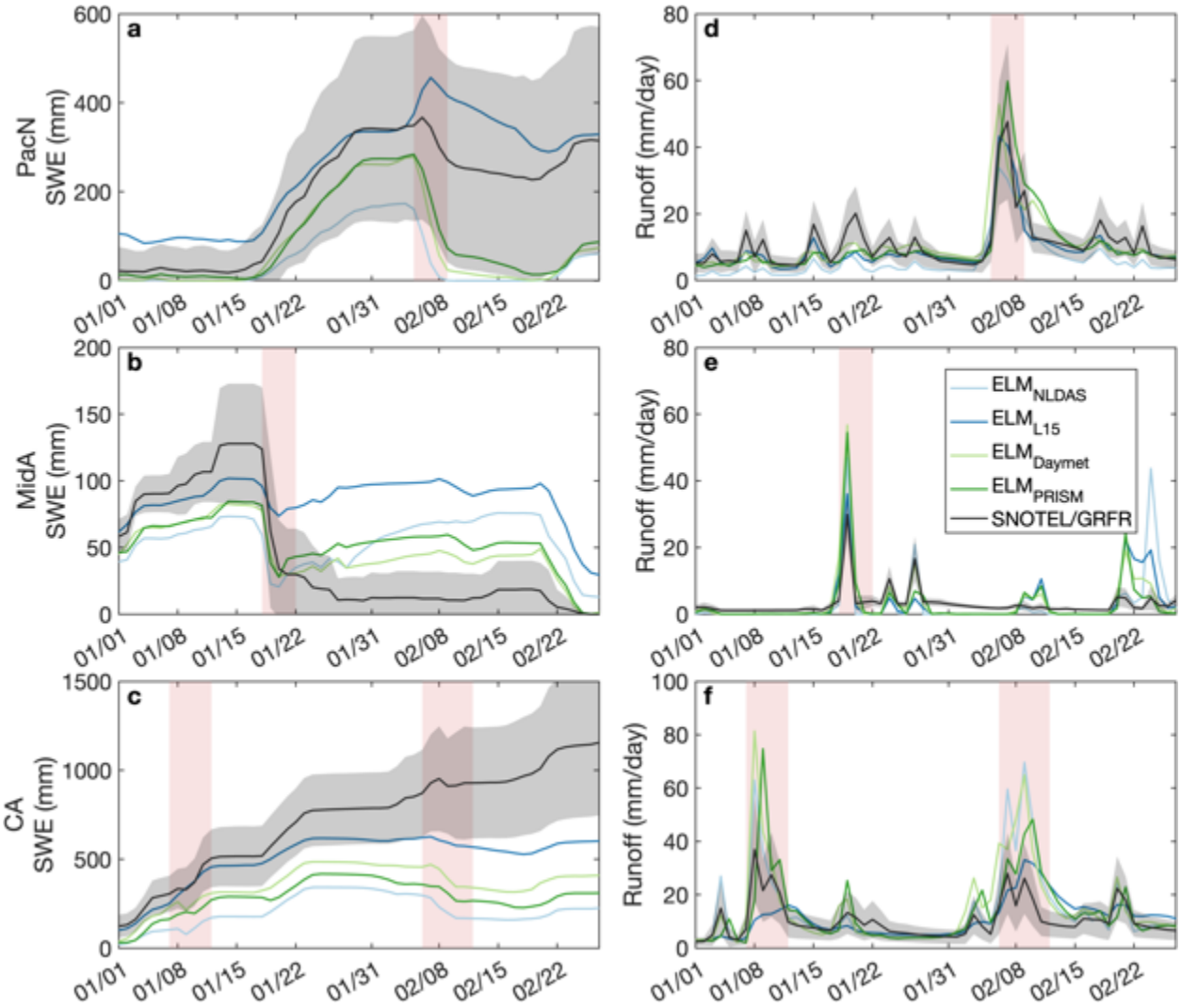

Supplementary Figure 2. Time series of ELM simulated and referenced snow water equivalent (SWE) and runoff for the ROS flood events over the three basins (PacN, MidA and CA). The default parameters were used in the ELM simulations. The referenced values are from the benchmark datasets in Table S1. In each panel, the black line and the width of the gray shading represent the mean and standard deviation of the referenced values, the colored lines represent the ELM simulated values, and the vertical pink shadings represent the periods of each ROS event. For the legend, the subscripts NLDAS, L15, Daymet and PRISM are four different atmospheric forcing datasets (Table S1), and SNOTEL and GRFR are the snow field measurements from the SNOTEL network and the Global Reach-level Flood Reanalysis runoff dataset. Since SNOTEL sites are only distributed in the western US, we used the daily Northern Hemisphere Snow Water Equivalent (NH-SWE) dataset for 1996MidA instead.

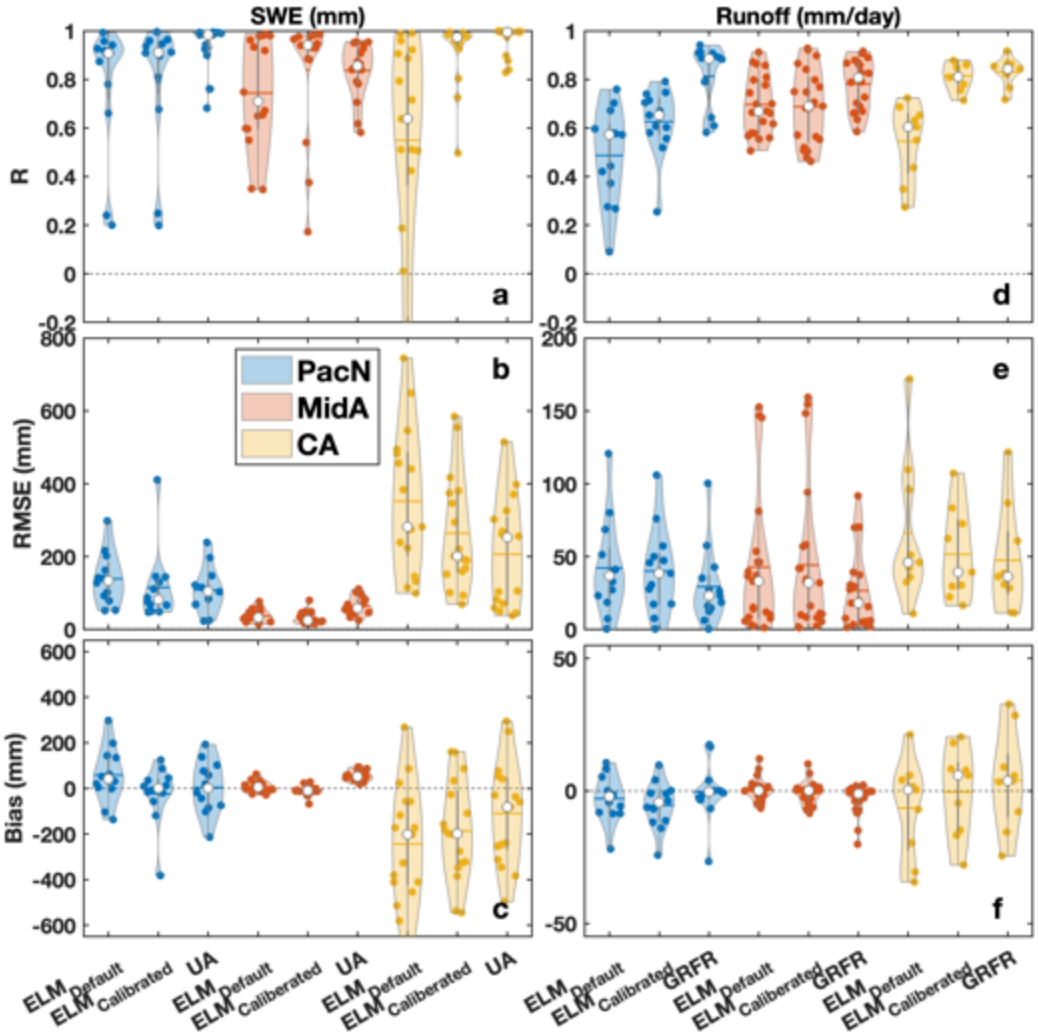

Supplementary Figure 3. Performance of ELM with the default and calibrated parameters and two comparable datasets (UA and GRFR) in capturing the snow water equivalent (SWE) and runoff represented in the benchmark datasets (i.e., the SNOTEL measurements and USGS streamflow observations) over the three basins (PacN, MidA, and CA), in terms of correlation coefficient (R), root mean square error (RMSE) and Bias at each site/basin. Note that the two months encompassing the events were selected (see Methods), and thus the two consecutive CA events are merged in the model evaluation over CA basin. In each panel, for the x-axis, $ELM_{Default}$ and $ELM_{Calibrated}$ are the ELM simulations with the default and calibrated parameters, respectively, and UA and GRFR are the SWE datasets developed by the University of Arizona and the Global Reach-level Flood Reanalysis runoff dataset, respectively; and for each violin plot, the white circle is the mean value, and each dot represents the metric at each SNOTEL site or USGS basin. Since SNOTEL sites are only distributed in the western US, we used the daily Northern Hemisphere Snow Water Equivalent (NH-SWE) dataset for 1996MidA instead.

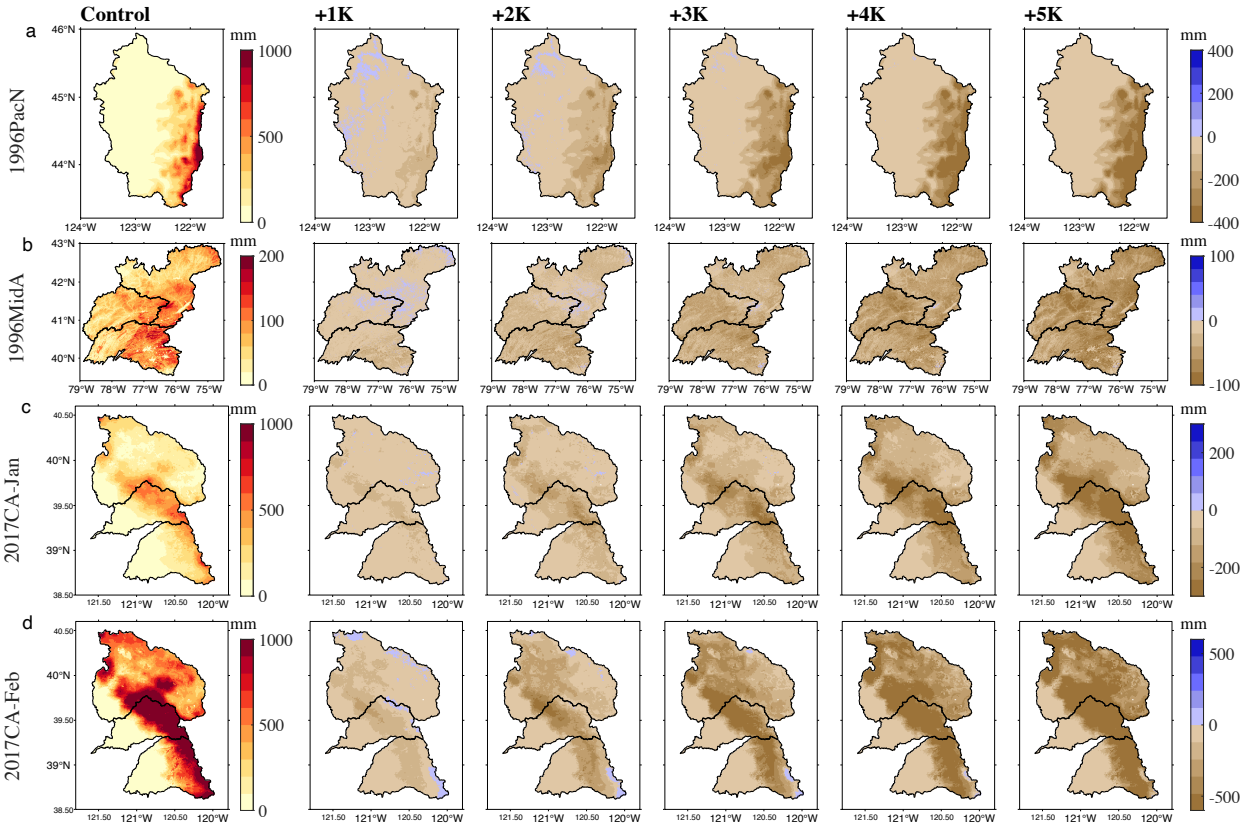

Supplementary Figure 4. Spatial distribution of initial snow water equivalent (SWE) before the ROS event, in the historical events and changes under a warmer climate. Panels a-d show four different events: 1996PacN, 1996MidA, 2017CA-Jan, and 2017CA-Feb. The first column is the historical simulation (Control), and the second to sixth columns are the differences between warming scenarios with the air temperature increasing from +1K to +5K and historical simulations.

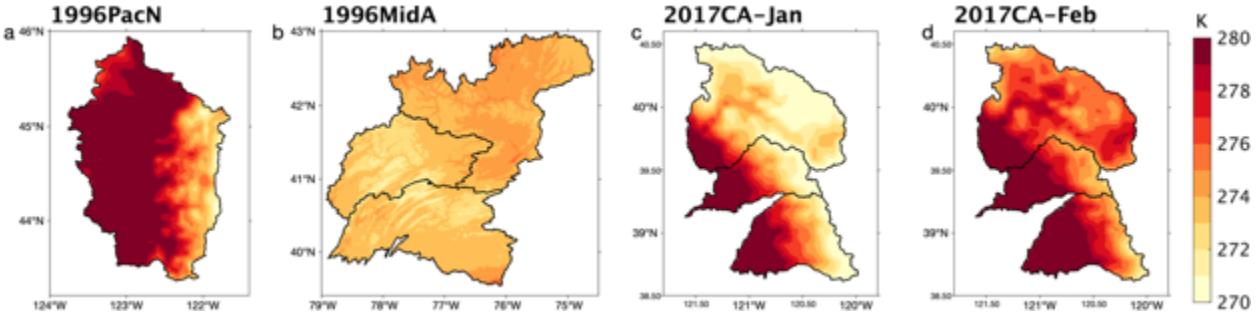

Supplementary Figure 5. Spatial distribution of average air temperature in the historical events. Panels a-d show four different events: 1996PacN, 1996MidA, 2017CA-Jan, and 2017CA-Feb.

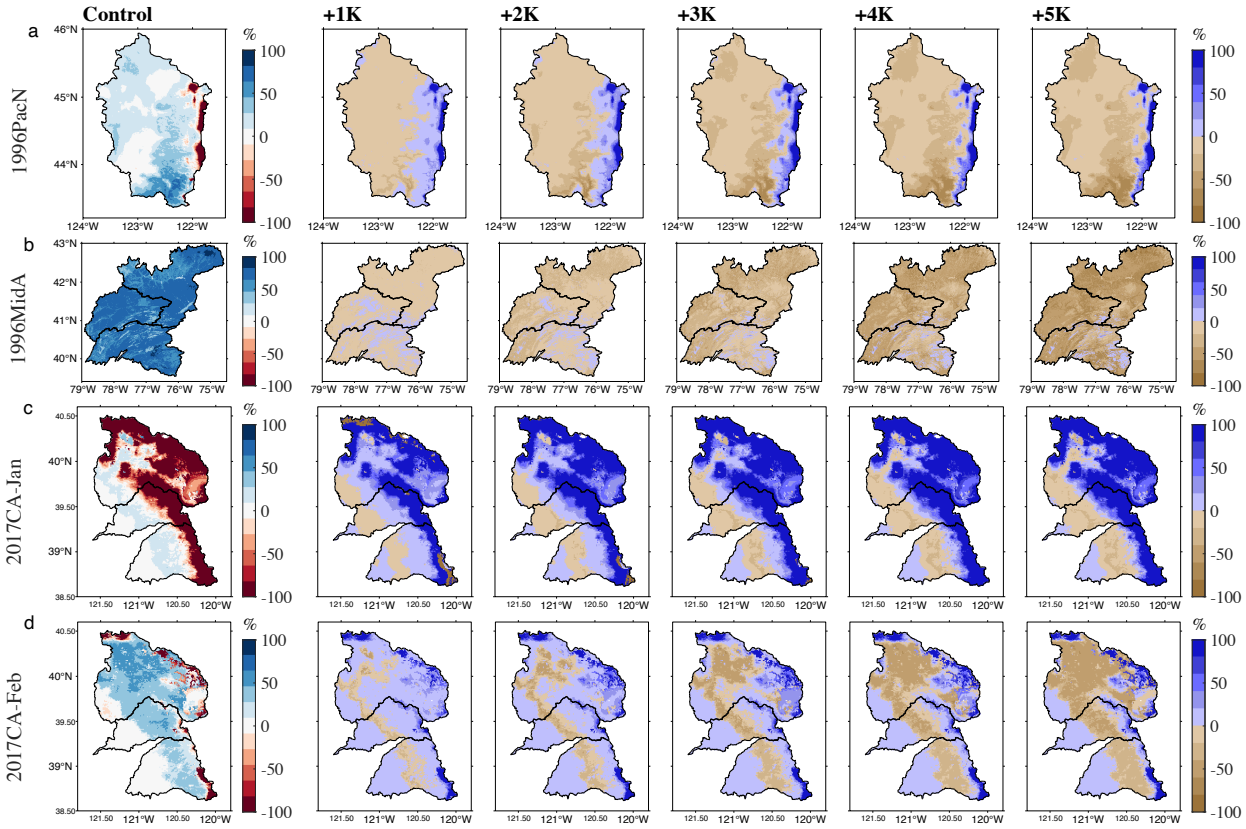

Supplementary Figure 6. Spatial distribution of relative snow contribution (C_{snow}) in the historical events and the changes under a warmer climate. Panels a-d show four different events: 1996PacN, 1996MidA, 2017CA-Jan, and 2017CA-Feb. The first column is the historical simulations (Control), and the second to sixth columns are the differences between warming scenarios with the air temperature increasing from +1K to +5K and the historical simulations.

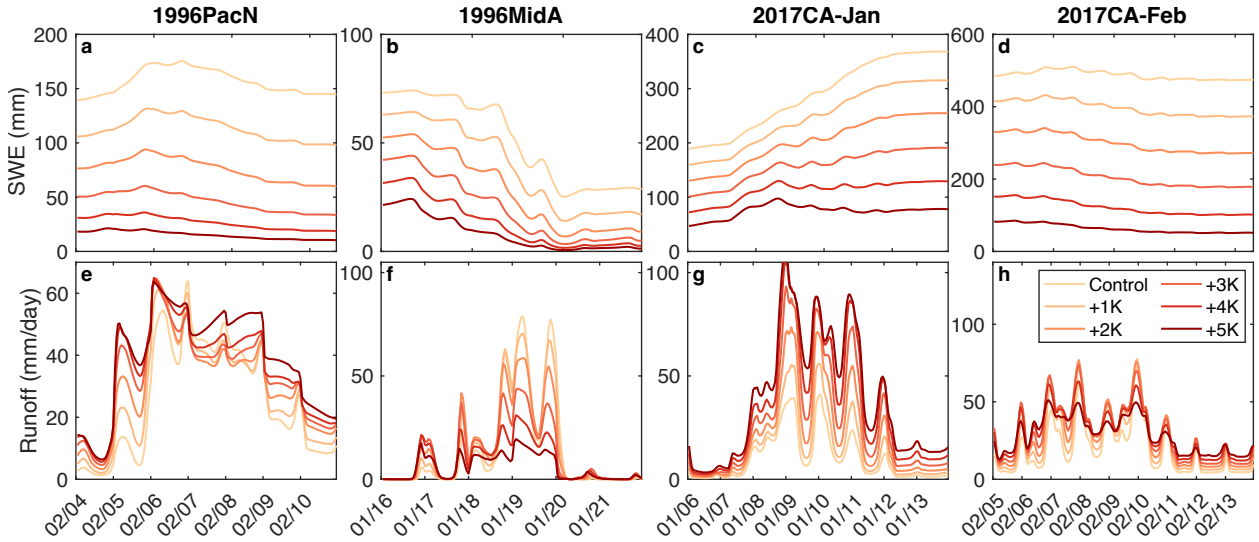

Supplementary Figure 7. Time series of basin average snow water equivalent (SWE) and runoff during the ROS flood events under the control and warming scenarios.

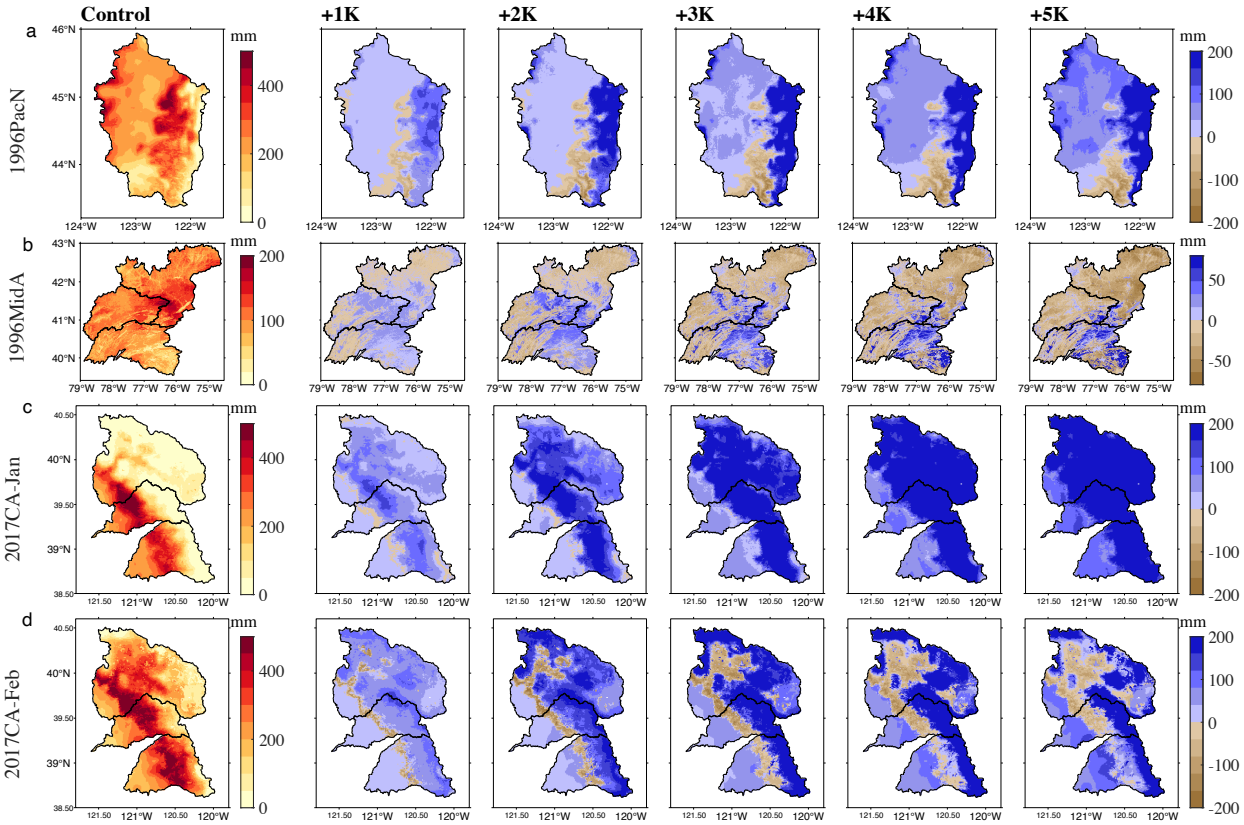

Supplementary Figure 8. Same as Figure S4, except for cumulative terrestrial water input (TWI).

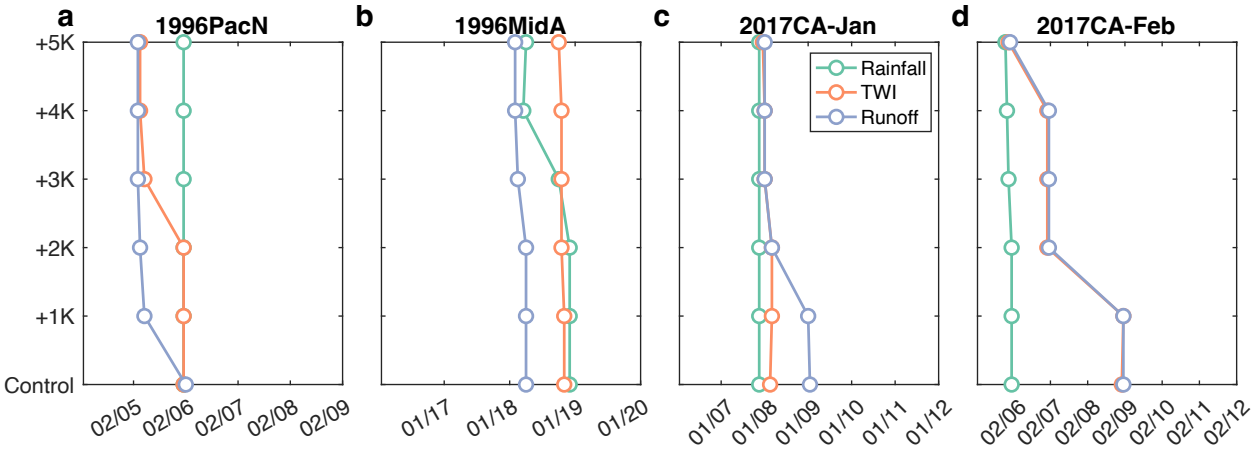

Supplementary Figure 9. The peaking time of rainfall, terrestrial water input (TWI), and runoff under the control and warming scenarios for the four events.

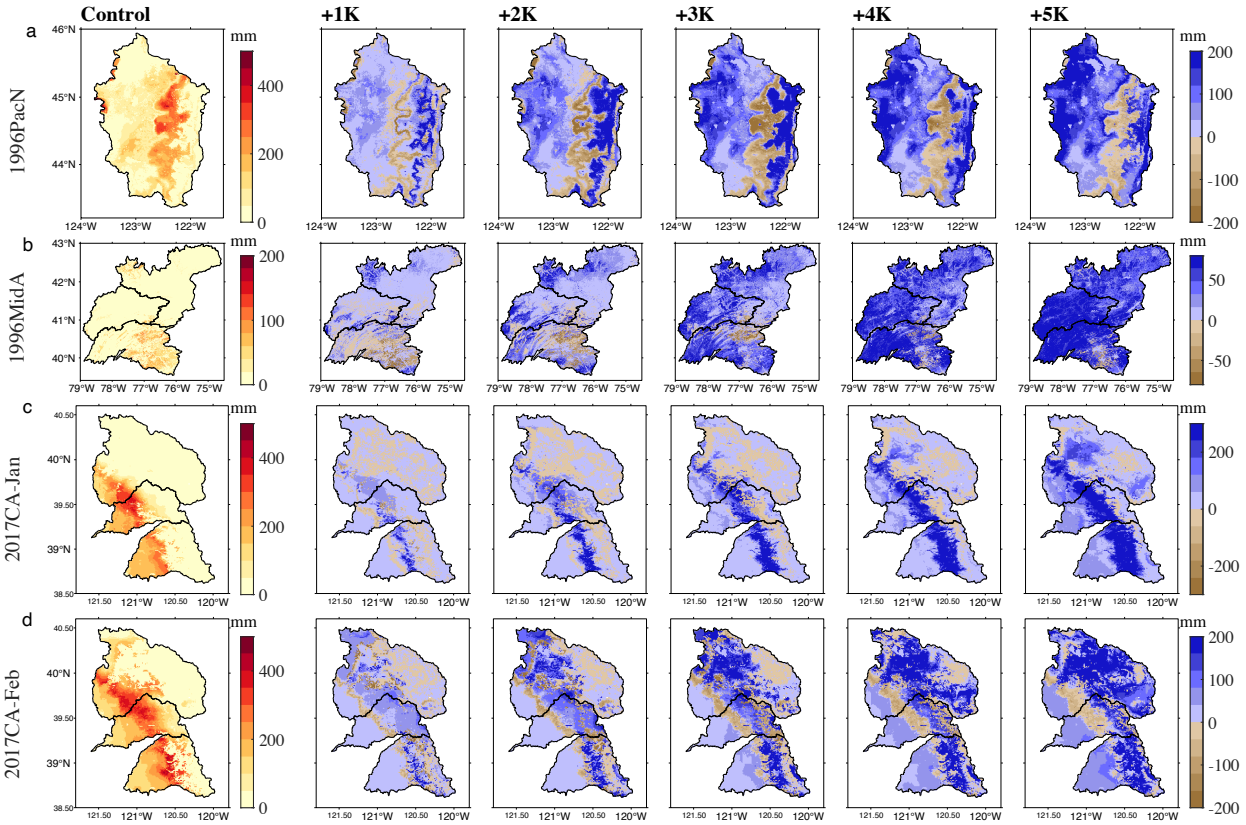

Supplementary Figure 10. Same as Figure S4, except for soil infiltration.

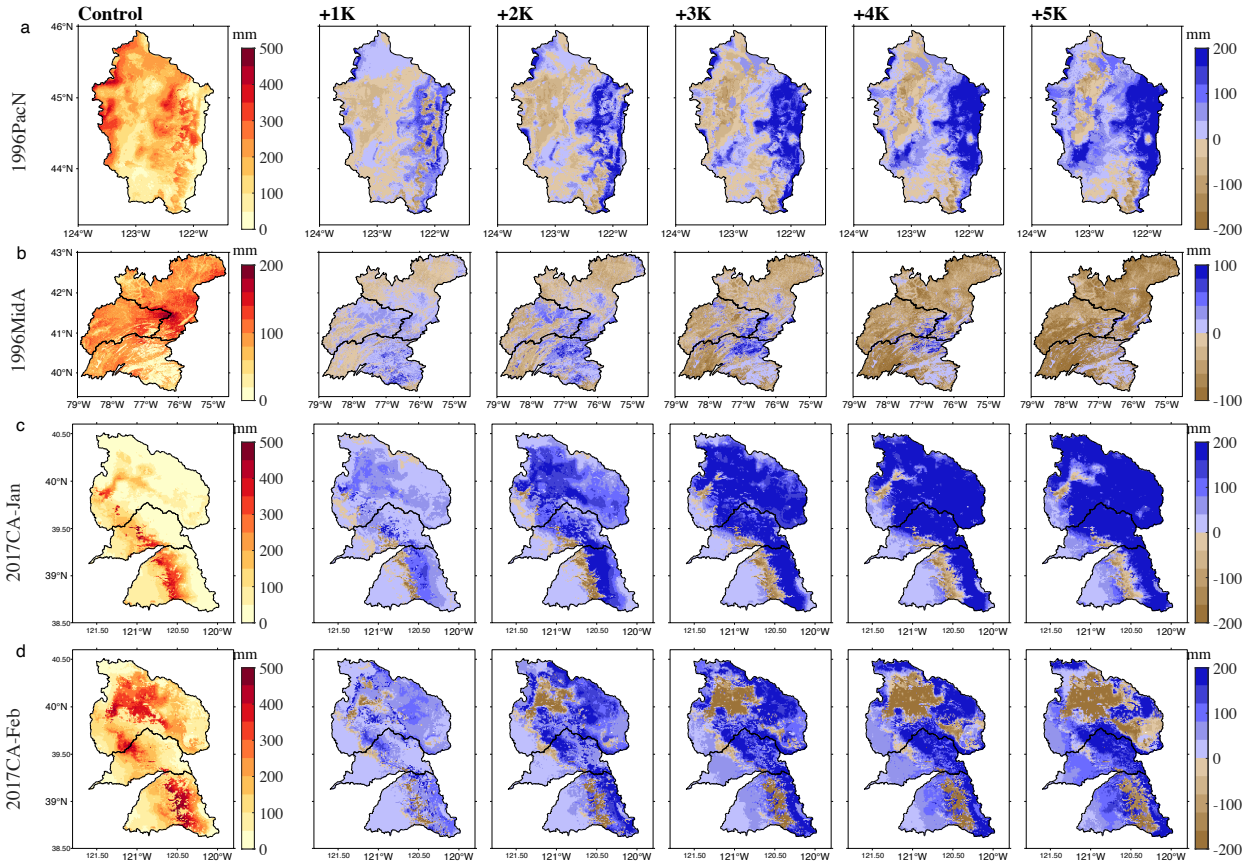

Supplementary Figure 11. Same as Figure S4, except for cumulative runoff.

Supplementary Figure 12. Spatial distribution of the sign changes in TWI and Runoff under a warmer climate. Panels a-d show four different events: 1996PacN, 1996MidA, 2017CA-Jan, and 2017CA-Feb, and the first to fifth columns are the sign changes in TWI and runoff under warming scenarios with the air temperature increasing from +1K to +5K compared to the historical simulations. In the legend, TWI+ and TWI- represent increasing and decreasing TWI, while Runoff+ and Runoff- represent increasing and decreasing runoff.

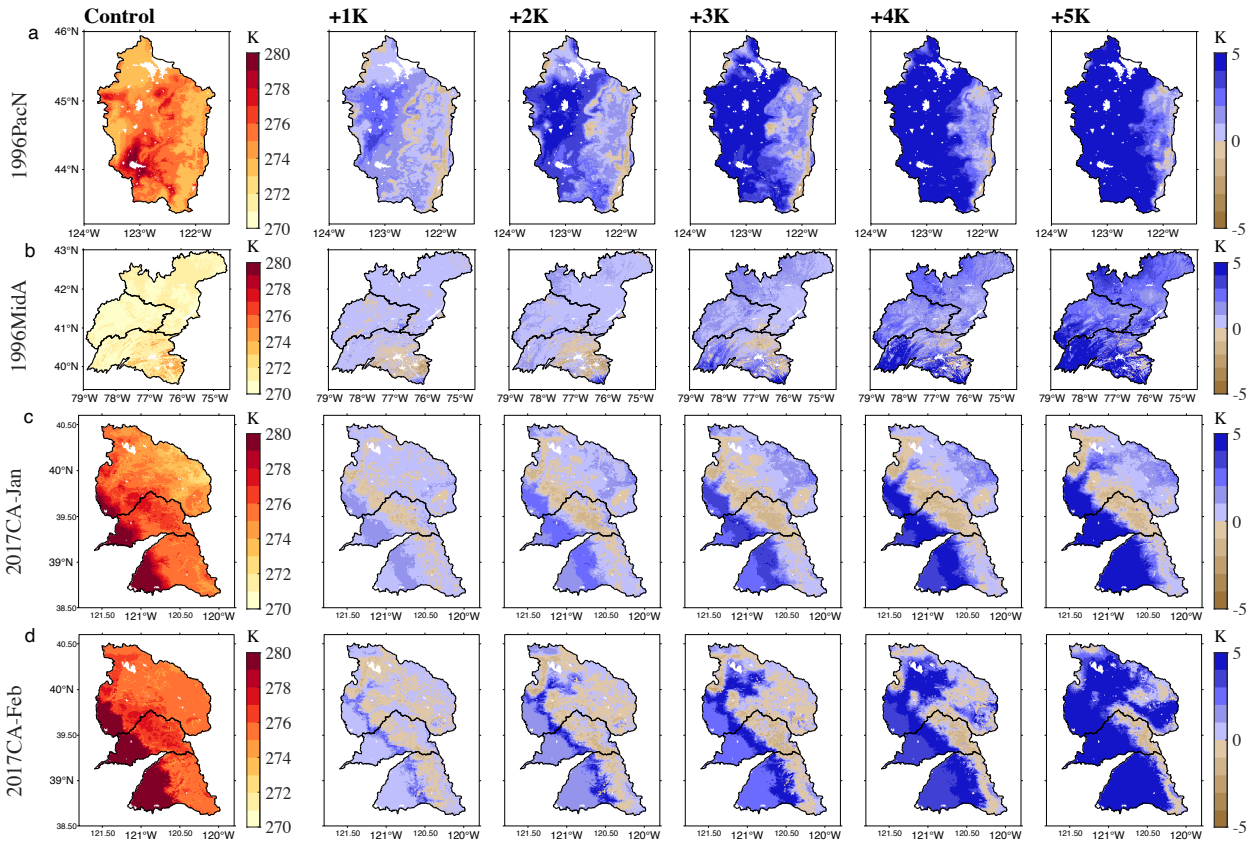

Supplementary Figure 13. Same as Figure S4, except for soil temperature in top 10 cm of soil.

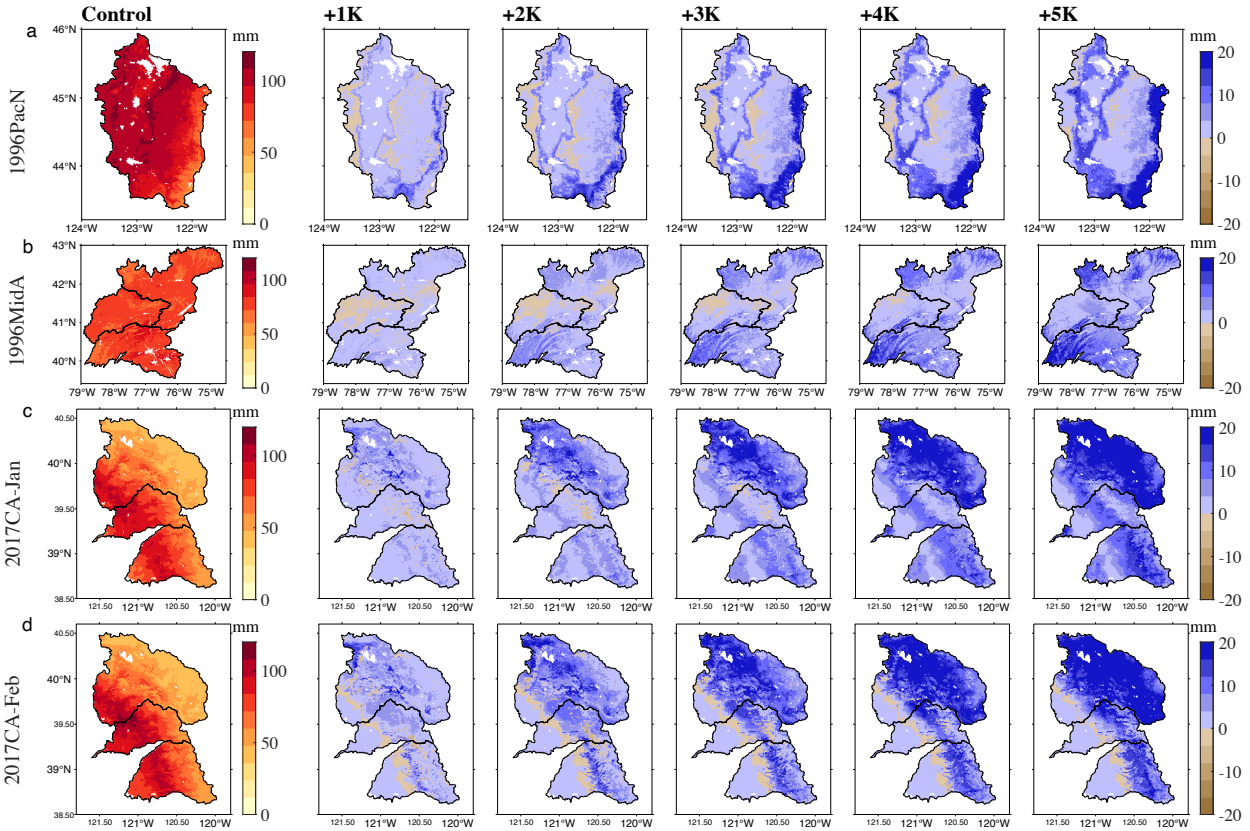

Supplementary Figure 14. Same as Figure S4, except for initial column-integrated soil moisture.

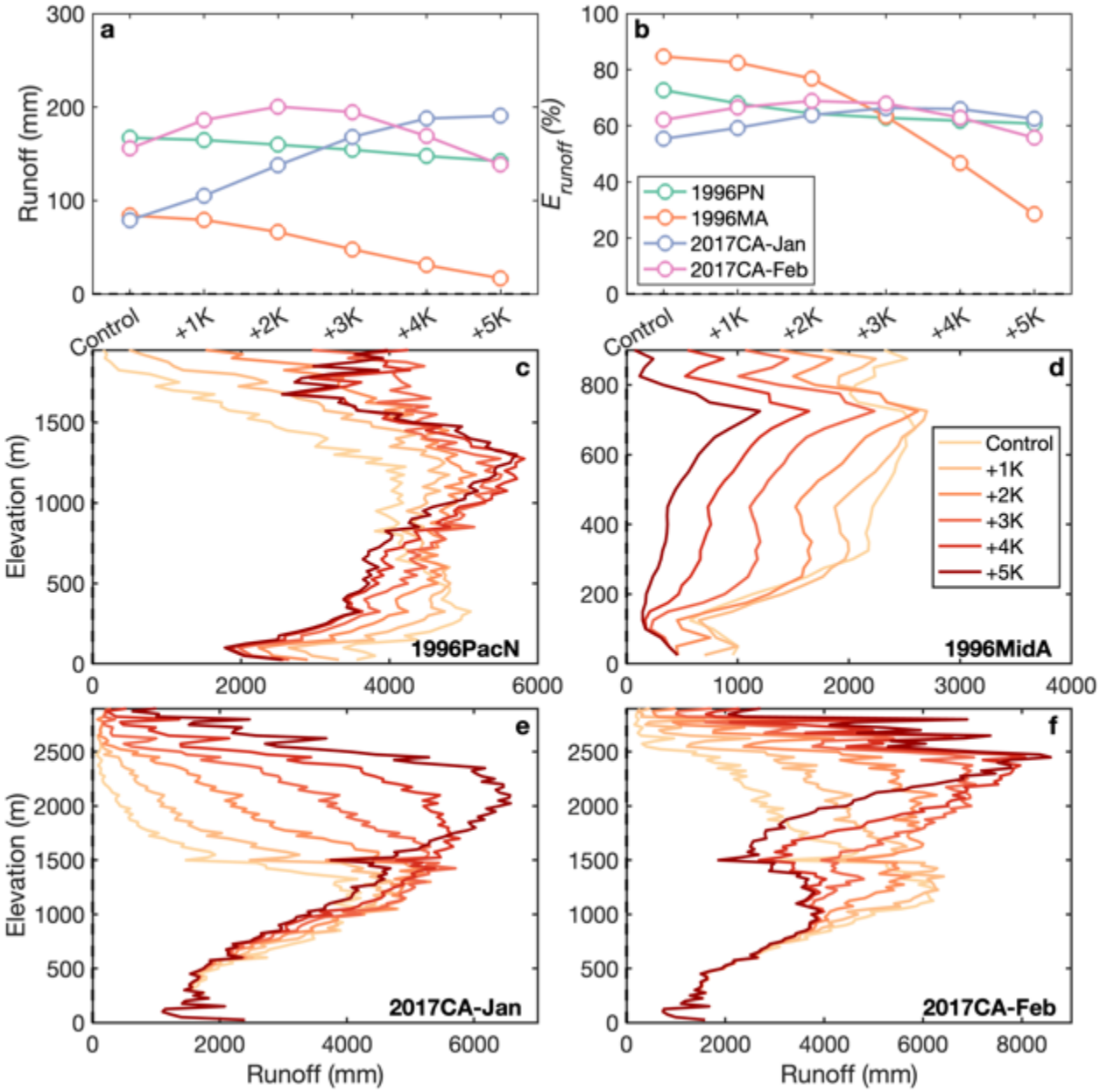

Supplementary Figure 15. Responses of the basin average and elevation profiles of cumulative runoff and runoff efficiency for the four events in a warmer climate without precipitation change. a, Basin average runoff under the control and warming scenarios without precipitation change. **b,** Basin average runoff efficiency, defined as the ratio of runoff to terrestrial water input (TWI), under the control and warming scenarios without precipitation change. **c-f,** Elevation profiles of runoff for the four events: 1996PacN, 1996MidA, 2017CA-Jan, and 2017CA-Feb.

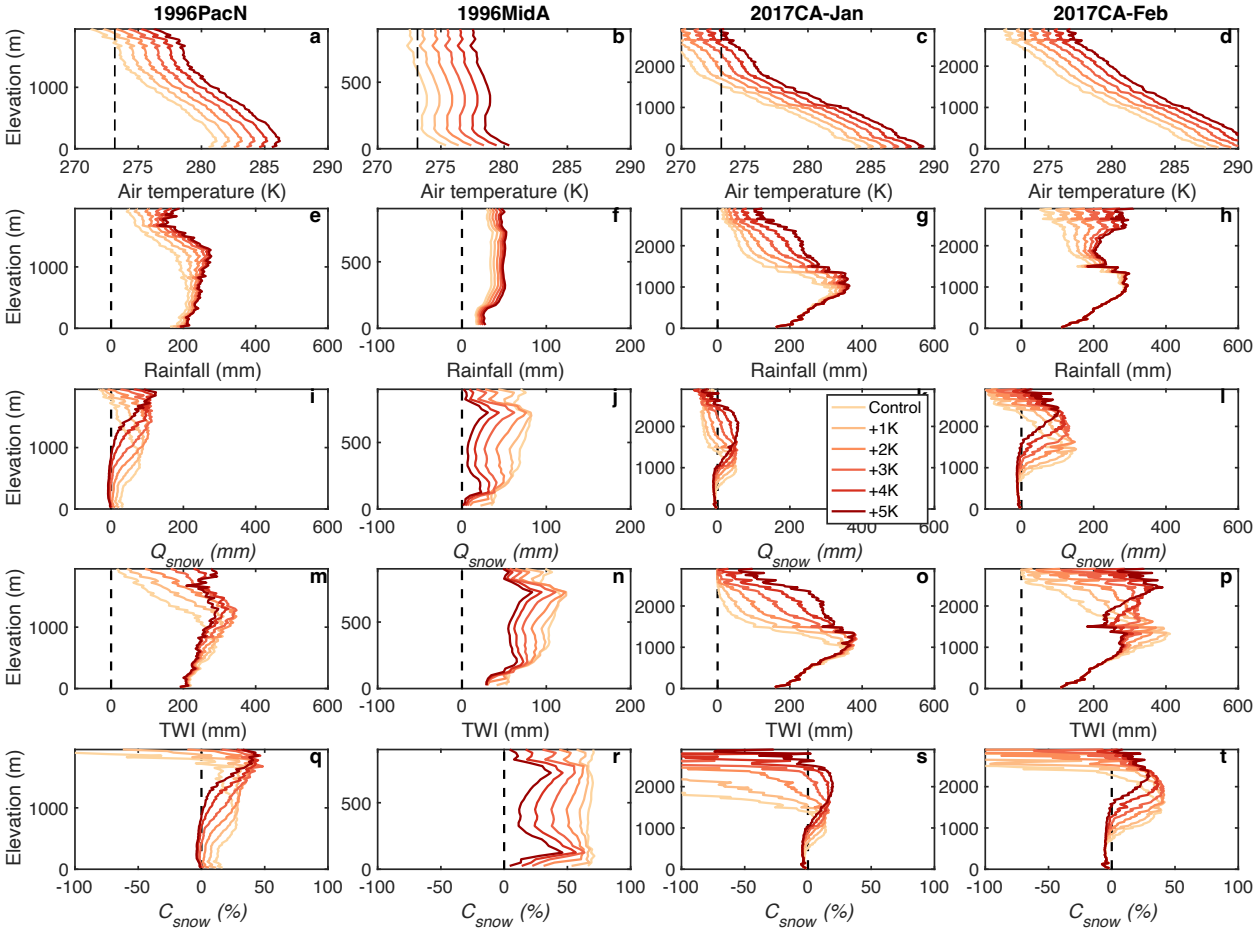

Supplementary Figure 16. Elevation profiles of different variables for the four events: 1996PacN, 1996MidA, 2017CA-Jan, and 2017CA-Feb under the control and warming scenarios without precipitation change**.** The first to fifth rows represent air temperature, rainfall, sum of liquid water retention and snowmelt (Q_{snow}), terrestrial water input (TWI), and **relative snow contribution to TWI (C_{snow})**, respectively.

Supplementary Table 1. Details of the used datasets in the study.

Category	Dataset	Spatial resolution	Temporal resolution	Reference	Download link
Meteorologic forcing	NLDAS-2	0.125 degree	Hourly	ref. (1)	https://disc.gsfc.nasa.gov/datasets?keywords=NLDAS
	L15	1/16 degree	Daily	ref. (2)	https://downloads.psl.noaa.gov/Datasets/livneh/fluxvars/
	PRISM	4 km	Daily	ref. (3)	https://prism.oregonstate.edu/recent/
	Daymet	1 km	Daily	ref. (4)	https://daymet.ornl.gov/
Snow water equivalent	SNOTEL	Site level	Daily	ref. (5)	https://www.pnnl.gov/data-products
	NH-SWE	Site level	Daily	ref. (6)	https://zenodo.org/records/7565252
	UA	4 km	Daily	ref. (7)	https://nsidc.org/data/nsidc-0719/versions/1
Runoff or streamflow	GRFR	5 km	Daily	ref. (8)	https://www.reachhydro.org/home/records/grfr
	USGS	Site level	Daily	ref. (9)	https://waterdata.usgs.gov
ELM	ELM	1 km	Half-hourly	This study	https://github.com/daleihao/ROS_Flood-Flood_Extremes

Supplementary Table 2. Performance of ELM with default and calibrated parameters driven by different atmospheric forcings in simulating snow water equivalent (SWE) and runoff. For the ELM case name, the subscript represents the atmosphere forcings, and the 'Optimal' represents the optimal atmospheric forcing with the best performance for each event (see Methods); and the superscript represents the default or calibrated parameters.

Region	Case	SWE (mm)			Runoff (mm/day)		
	Metric	R	RMSE	Bias	R	RMSE	Bias
PacN	$ELM_{NLDAS}^{Default}$	0.41	259.7	-162.4	0.88	6.2	-4.8
	$ELM_{L15}^{Default}$	0.75	155.7	58.7	0.90	4.0	-1.8
	$ELM_{Daymet}^{Default}$	0.52	227.5	-126.3	0.78	5.6	0.0
	$ELM_{PRISM}^{Default}$	0.65	206.1	-114.4	0.86	5.3	-0.4
	$ELM_{Optimal}^{Calibrated}$	0.77	150.0	-24.1	0.92	4.7	-2.7
MidA	$ELM_{NLDAS}^{Default}$	0.24	62.6	17.7	0.75	6.9	0.1
	$ELM_{L15}^{Default}$	0.32	87.3	50.0	0.65	5.3	0.0
	$ELM_{Daymet}^{Default}$	0.60	41.4	7.0	0.88	5.3	0.4
	$ELM_{PRISM}^{Default}$	0.55	46.4	14.4	0.82	5.3	-0.2
	$ELM_{Optimal}^{Calibrated}$	0.72	36.3	-9.0	0.91	5.1	0.1
CA	$ELM_{NLDAS}^{Default}$	0.35	655.0	-563.2	0.86	10.5	3.8
	$ELM_{L15}^{Default}$	0.53	398.6	-243.9	0.49	7.0	0.9
	$ELM_{Daymet}^{Default}$	0.60	494.9	-406.4	0.87	11.6	5.2
	$ELM_{PRISM}^{Default}$	0.29	597.2	-481.8	0.66	10.8	3.4
	$ELM_{Optimal}^{Calibrated}$	0.72	304.5	-186.8	0.86	6.7	1.8

Supplementary Table 3. Information on the sensitive parameters in the ELM calibration.

Category	Parameter	Unit	Definition	Default value	Range
Snow	C_a	Unitless	Tunning parameter for top snow/soil layer thickness	0.34	[0.0, 1.0]
	T_{fall}	K	Snowfall temperature	274.15	[273.15, 275.15]
	K_{accum}	Unitless	Snow cover accumulation parameter	0.1	[0.02, 0.4]
	N_{melt}	Unitless	Snow cover depletion curve shape parameter	200.0	[50, 400]
	T_{free}	K	Snow freezing temperature	273.15	[271.15, 275.15]
Runoff	f_{over}	m^{-1}	Decay factor for surface runoff	0.5	[0.1, 5]
	f_{drai}	m^{-1}	Decay factor for subsurface runoff	2.5	[0.1, 5]

SI References

1. Y. Xia, K. Mitchell, M. Ek, J. Sheffield, B. Cosgrove, E. Wood, L. Luo, C. Alonge, H. Wei, J. Meng, B. Livneh, D. Lettenmaier, V. Koren, Q. Duan, K. Mo, Y. Fan, D. Mocko, Continental-scale water and energy flux analysis and validation for the North American Land Data Assimilation System project phase 2 (NLDAS-2): 1. Intercomparison and application of model products. *Journal of Geophysical Research: Atmospheres* **117**, (2012).

2. B. Livneh, T. J. Bohn, D. W. Pierce, F. Munoz-Arriola, B. Nijssen, R. Vose, D. R. Cayan, L. Brekke, A spatially comprehensive, hydrometeorological data set for Mexico, the U.S., and Southern Canada 1950–2013. *Scientific Data* **2**, 150042 (2015).

3. C. Daly, R. P. Neilson, D. L. Phillips, A Statistical-Topographic Model for Mapping Climatological Precipitation over Mountainous Terrain. *Journal of Applied Meteorology and Climatology* **33**, 140-158 (1994).

4. P. E. Thornton, S. W. Running, M. A. White, Generating surfaces of daily meteorological variables over large regions of complex terrain. *Journal of Hydrology* **190**, 214-251 (1997).

5. N. Sun, H. Yan, M. S. Wigmosta, L. R. Leung, R. Skaggs, Z. Hou, Regional Snow Parameters Estimation for Large-Domain Hydrological Applications in the Western United States. *Journal of Geophysical Research: Atmospheres* **124**, 5296-5313 (2019).

6. A. Fontrodona-Bach, B. Schaefli, R. Woods, A. J. Teuling, J. R. Larsen, NH-SWE: Northern Hemisphere Snow Water Equivalent dataset based on in situ snow depth time series. *Earth Syst. Sci. Data* **15**, 2577-2599 (2023).

7. X. Zeng, P. Broxton, N. Dawson, Snowpack Change From 1982 to 2016 Over Conterminous United States. *Geophysical Research Letters* **45**, 12,940-912,947 (2018).

8. Y. Yang, M. Pan, P. Lin, H. E. Beck, Z. Zeng, D. Yamazaki, C. H. David, H. Lu, K. Yang, Y. Hong, E. F. Wood, Global Reach-Level 3-Hourly River Flood Reanalysis (1980–2019). *Bulletin of the American Meteorological Society* **102**, E2086-E2105 (2021).

9. J. A. Falcone, "GAGES-II: Geospatial attributes of gages for evaluating streamflow" (US Geological Survey, 2011).